EUROPEAN ORGANIZATION FOR NUCLEAR RESEARCH

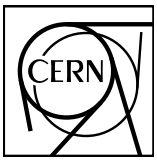

CERN-EP–2019-xxx
November 19, 2019

Long-range correlations in high-multiplicity proton–proton collisions at $\sqrt{s}$ = 13 TeV with ALICE at the LHC

Abstract

The observed azimuthal modulations of long-range correlations in pseudorapidity in small systems like pp or p-Pb collisions show strikingly similar features to those seen in heavy ion collisions. Many theoretical approaches to interpreting this effect have been developed. However, it is still unclear whether these long-range correlations are due to final or initial state effects. To further investigate these effects, we studied long-range correlations as a function of transverse momentum in very high multiplicity pp collisions at $\sqrt{s} = 13$ TeV, collected with the high multiplicity event trigger during 2016 and 2017 with ALICE. In this talk, we present the near-side per-trigger yield at large pseudorapidity separation (ridge yield) as a function of transverse momentum in pp collisions at $\sqrt{s} =$ 13 TeV. The results are compared to previous measurements from CMS and ATLAS experiments. In addition, we present the ridge yield in events where harder fragmentation processes are present, to explore possible physical origins of long-range correlations.

1 Introduction

Collective effects are one of the key probes to study evolution of the hot and dense matter created in ultra-relativistic heavy-ion collisions. The enhancement in the associated yield of two-particle correlations at small relative azimuthal angle ($\Delta\varphi$) that extends over a long-range of relative pseudorapidity ($\Delta\eta$), often referred to as the "ridge", is one of the crucial observables of collectivity [1, 2]. In recent years, measurements of the ridge in small systems, such as proton-proton (pp) collisions and proton-nucleus (pA) collisions, where the volume and lifetime of the medium produced are expected to be small, have been reported[3–6]. There are many theoretical attempts[7–10] to interpret the ridge considering hydrodynamics, saturation or other mechanisms, but a quantitative description of the full set of experimental data has not yet been achieved.

2 Experimental setup

Delivery of protons with world-highest energy by LHC at CERN makes it possible to generate various phenomena from their collisions. Recent center-of-mass energy of colliding two protons is increased up to $\sqrt{s} = 13$ TeV during LHC Run2 period. Among data from proton-proton collisions at 13 TeV, This paper describes analysis results obtained by using 2016 to 2018 data sets.

The full description of ALICE detector in the LHC Run 2 can be found in Ref. [11]. The present analysis mainly uses V0([13]), ITS (Inner Tracking System, [12]) and TPC (Time Projection Chamber, [14]) detectors. The V0 detector consists of two rings, V0-A and V0-C, each made of 32 scintillator tiles, covering the full azimuthal angle within 2.8$< \eta <$5.1 and -3.7$< \eta <$-1.7, respectively. The V0 provides trigger and estimation of event multiplicity. A sample of events with high numbers of produced particles is obtained with a high multiplicity trigger in the V0 detector.

The responsibility of reconstruction of charged track is up to the ITS and the TPC. The ITS is composed of three subsystems, Silicon Pixel Detector(SPD), Silicon Drift Detector (SDD) and Silicon Strip Detector (SSD). The ITS has an acceptance up to $|\eta| <$1.95 for single charged track reconstruction. The TPC, which is working inside solenoidal magnetic field of 0.5 T, has an acceptance up to $|\eta| <$0.9 for charged tracks reaching the outer radius of the TPC. The tracking of charged-particles is done with the combination of the ITS and the TPC, which enable the reconstruction of tracks down to 0.2 GeV/c with $\sim$75% efficiency.

3 Analysis

The multiplicity class used in the present analysis is top 0-0.1%, which denotes the most particle-abundant events, to study high multiplicity events and to observe the ridge structure. This analysis uses charged tracks, whose reconstructed transverse momentum is larger than 0.2 GeV/c in a fiducial region as $|\eta| <$0.9. The efficiency and contamination from non-primary tracks are estimated from a Monte Carlo simulation with PYTHIA8 event generator and with particle transport through the detector using GEANT simulation.

The two-particle correlation between trigger particle and associated particle is measured as function of relative pseudorapidity and azimuthal angle. The following equation expresses the correlation as associated yield per trigger particle as function of transverse momentum($p_{\mathrm{T,trig}}$, $p_{\mathrm{T,assoc}}$) of trigger particle and associated particle with the condition of $p_{\mathrm{T,trig}} > p_{\mathrm{T,assoc}}$

$$\frac{1}{N_{\mathrm{trig}}} \frac{\mathrm{d}^2 N_{\mathrm{assoc}}}{\mathrm{d}\Delta\eta\,\mathrm{d}\Delta\varphi} = B(0,0)\frac{S(\Delta\eta,\Delta\varphi)}{B(\Delta\eta,\Delta\varphi)}, \tag{1}$$

where the N_{trig} is the number of trigger particles in the corresponding event class. The signal distribution $S(\Delta\eta,\Delta\varphi)$ is constructed using two-particle correlation in the same event. The background distribution

$B(\Delta\eta,\Delta\varphi)$ is constructed using two-particle correlation in mixed several events having the same primary vertex and belonging to the same multiplicity class.

The quantitative study of ridge is done with $\Delta\varphi$ distribution at large $\Delta\eta$ to allow direct comparison of ridges between different p_{T} intervals. The large $\Delta\eta$ range is defined as $1.5< |\Delta\eta| <1.8$ considering the limited detector acceptance. The baseline of the correlations is subtracted by implementing Zero-Yield-At-Minimum (ZYAM) procedure. The minimum yield (C_{ZYAM}) is defined as minimum value of the function, which consists of Fourier series up to the third harmonic and is determined by fitting the $\Delta\varphi$ distribution. By subtracting C_{ZYAM} from the $\Delta\varphi$ distribution, the magnitude of long-range near-side yield is obtained and can be quantified by integrating the near-side peak of the $\Delta\varphi$ distribution. The range of integration is enclosed by the points having the minimum yield, which is obtained from ZYAM procedure.

The ridge yield is further studied with various event selections regarding hard processes. The event selection is implemented by requiring that transverse momentum of leading track is larger than specific threshold. The leading track is defined as a charged track having the largest transverse momentum in a given event. Because the high transverse momentum track mainly comes from hard scattering, the requirement of the leading track can control the hardness of events, which allow one to study the ridge with events containing hard scatterings.

4 Results

The two-dimensional associated yield per trigger particle is shown in Figure 1 for pairs of trigger particle and associated particle with $1.0< p_{\mathrm{T,assoc}} < p_{\mathrm{T,trig}} <2.0$ GeV/c in pp collisions at $\sqrt{s}$ =13 TeV in the 0-0.1% (left), 5-20% (middle) and 20-100% (right) multiplicity class estimated by V0 detector, which covers forward rapidity region. The ridge is clearly seen in high multiplicity class unlike in lower multiplicity classes.

The one-dimensional $\Delta\varphi$ distribution is shown in Figure 2 for pairs of particles with various p_{T} intervals in very high multiplicity class. The associated yield per trigger particle is compared with CMS results. The near-side peak is highest in the $1.0< p_{\mathrm{T}} <2.0$ interval and gradually decreases with increasing p_{T}.

The spectra of the ridge yield is shown in Figure 3 in very high multiplicity class and compared with CMS results. The estimator of particle multiplicity of ALICE is done with forward subsystem(V0), whereas that of CMS is done by mid-rapidity particles meeting with the condition of $|\eta| <2.4$ and $p_{\mathrm{T}} >0.4$ GeV/c. Dedicated comparison is conducted and the difference of particle multiplicity is estimated to be about 20%. Taking into account the difference in acceptance of charged tracks and comparable definition of multiplicity,, the measurements are can be considered comparable with each other.

To further understand the behavior of the ridge in events including hard processes, the two-dimensional

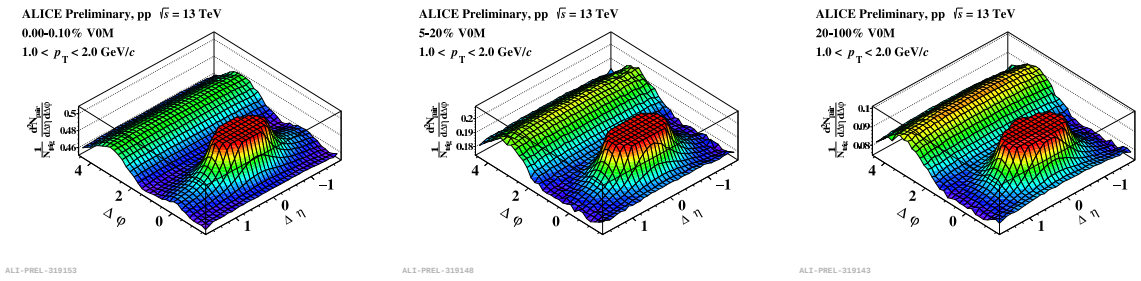

Fig. 1: Two-dimensional associated yield per trigger particle as function of $\Delta\eta$ and $\Delta\varphi$ in 0-0.1% (left), 5-20% (middle) and 20-100% (right) multiplicity class. The interval of transverse momentum of trigger particle and associated particle is $1.0< p_{\mathrm{T}} <2.0$ GeV/c.

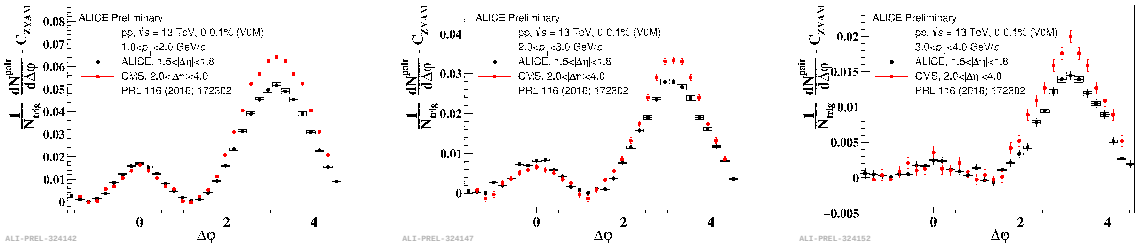

Fig. 2: One-dimensional $\Delta\varphi$ distribution in the large $\Delta\eta$ with various transverse momentum intervals. Interval of transverse momentum of trigger particle and associated particle is 1.0< p_{T} <2.0 GeV/c (left), 2.0< p_{T} <3.0 GeV/c (middle) and 3.0< p_{T} <4.0 GeV/c (right), respectively.

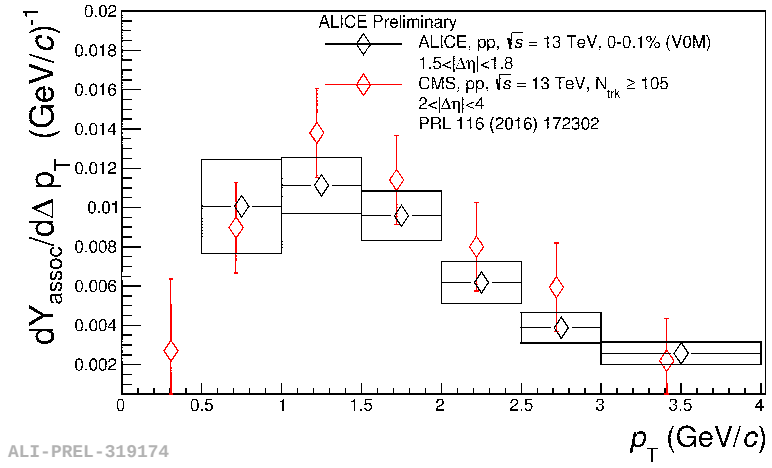

Fig. 3: (color online) The spectra of ridge yield as function of transverse momentum. The spectrum is compared with CMS result [3].

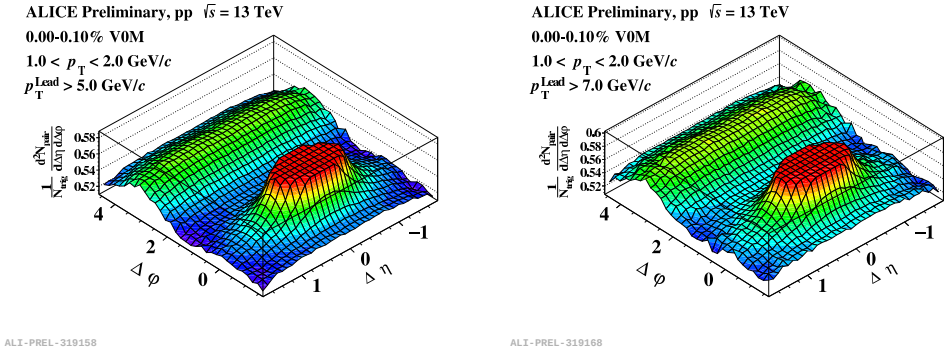

Fig. 4: Two-dimensional associated yield per trigger particle as function of $\Delta\eta$ and $\Delta\varphi$ in top 0-0.1% multiplicity class. The interval of transverse momentum of trigger particle and associated particle is 1.0< p_{T} <2.0 GeV/c for the plots. Threshold for leading track selection is 5 GeV/c (left) and 7 GeV/c (right), respectively.

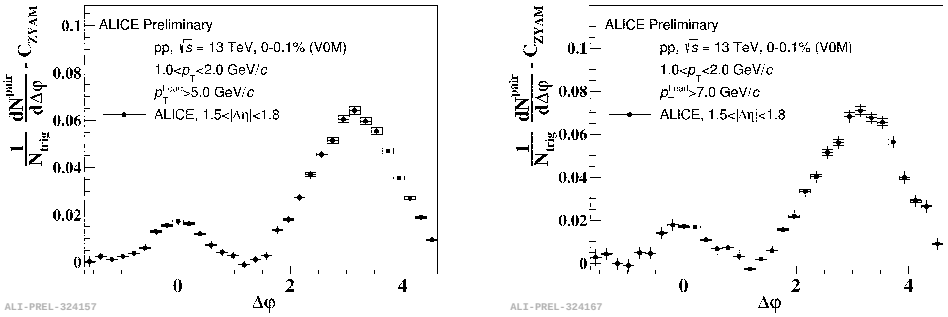

Fig. 5: One-dimensional $\Delta\varphi$ distribution in the large $\Delta\eta$ with various leading track selection thresholds. Interval of transverse momentum of trigger particle and associated particle is $1.0< p_{\mathrm{T}} <2.0$ GeV/c. Threshold for leading track selection is 5 GeV/c (left) and 7 GeV/c (right) respectively.

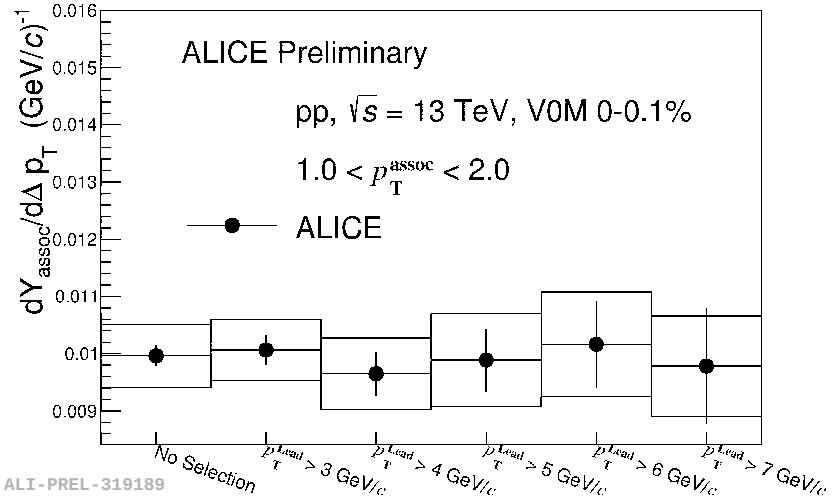

Fig. 6: The ridge yield spectrum with respect to the leading tracçk selection. The ridge yields are identical within uncertainties.

associated yield per trigger particle is measured with the leading track selection as shown in Figure 4. The ridge is still visible in the events where $p_{\mathrm{T}}^{\mathrm{Lead}}$ >7 GeV/c, which means that the ridge co-exists with hard-scattering in pp collisions.

The one-dimensional $\Delta\varphi$ distribution with the leading track selection is shown in Figure 5. The near-side yield doesn't change with respect to the leading track requirements within the uncertainties, whereas the away-side peak increases as the leading track requirement gets stronger, presumably because of the increase of the recoil jet yield.

The ridge yield is inspected as a function of the leading track selection in Figure 6. As seen in the previous plots, the ridge yield does not depend on the selection, which indicates that the ridge is not affected significantly by the hardness of the events.

5 Model Comparison

6 Conclusions

Two-particle angular correlations in large $|\Delta\eta|$ has been measured in very high multiplicity events in pp collsions at $\sqrt{s} = 13$ TeV with ALICE. The measured associated yield is found to be consistent with the previous results from CMS experiment. The ridge yield, for the first time, has been observed in events including hard processes. Furthermore, it is found to be independent of the hardness of the events. This observation is important for the study of the origins of the ridge in small collision systems.

References

[1] CMS Collaboration, "Centrality dependence of dihadron correlations and azimuthal anisotropy harmonics in PbPb collisions at $\sqrt{s_{\rm NN}}$ =2.76 TeV", Eur. Phys J. C72 (2012).

[2] ALICE Collaboration, "Anisotropic Flow of Charged Particles in Pb-Pb Collisions at $\sqrt{s_{\rm NN}}$ =5.02 TeV", Phys. Rev. Lett. 116, 132302 (2016).

[3] CMS Collaboration, Measurement of Long-Range Near-Side Two-Particle Angular Correlations in pp Collisions at $\sqrt{s}$ =13 TeV", Phys. Rev. Lett. 116, 172302 (2016).

[4] CMS Collaboration, "Evidence for collectivity in pp collisions at the LHC", Phys. Lett. B765 (2017) 193.

[5] ALICE Collaboration, "Investigations of anisotropic flow using multi-particle azimuthal correlations in pp, p-Pb, Xe-Xe, and Pb-Pb collisions at the LHC", arXiv:1903.01790 [nucl-ex].

[6] PHENIX Collaboration, "Creation of quark–gluon plasma droplets with three distinct geometries", Nature Phys. 15, 214 (2019), Nature Phys. 13, 535.

[7] H. Mäntysaari, B. Schenke, C. Shen and P. Tribedy, "Imprints of fluctuating proton shapes on flow in proton-lead collisions at the LHC", Phys. Lett. B772 (2017) 681.

[8] W. Zhao, Y. Zhou, H. Xu, W. Deng, and H. Song, "Hydrodynamic collectivity in proton?proton collisions at 13 TeV," Phys. Lett. B780 (2018) 495.

[9] K. Welsh, J. Singer, and U. W. Heinz, "Initial state fluctuations in collisions between light and heavy ions," Phys. Rev. C94 no. 2, (2016) 024919.

[10] M. Greif, C. Greiner, B. Schenke, S. Schlichting, and Z. Xu, "Importance of initial and final state effects for azimuthal correlations in p+Pb collisions," Phys. Rev. D96 no. 9, (2017) 091504.

[11] ALICE Collaboration, "The ALICE experiment at the CERN LHC," JINST 3 (2008) S08002.

[12] ALICE Collaboration, "Performance of the present ALICE Inner Tracking System and studies for the upgrade", Journal of Instrumentation, 7, June (2012) C06007.

[13] ALICE Collaboration, "Performance of the ALICE VZERO system", JINST 8 (2013) P10016.

[14] ALICE Collaboration, "Performance of the ALICE Time Projection Chamber", Physics Procedia 37, (2012) 434.